Simulation of Biogenic Carbon Capture and Utilization Process Chain

K. Tiiro. M. Ohenoja. O. Ruusunen. R. L. Keiski. M. Ruusunen

Environmental and Chemical Engineering Research Unit, University of Oulu, 90570 Oulu, Finland, (e-mail: forename.surname@oulu.fi).

Abstract: Carbon capture and utilization (CCU) is a growing field in chemical engineering with high expectations to replace fossil carbon. This paper focuses on modeling and simulation of a CCU process chain utilizing biogenic CO_2. A scenario with a pulp mill recovery boiler effluent is assumed. CO_2 capture is performed with a membrane-based system. This is followed by methanol synthesis, and the majority of produced methanol is directed to dimethyl carbonate (DMC) synthesis.

The process chain with fixed process design was simulated for different scenarios of the flue gas properties. The key process indicators were observed. Further, the flexibility of the processes was evaluated to mitigate the changes in process indicators due to fluctuating flue gas properties. Finally, model parameter uncertainties and modeling assumptions were discussed. The results indicate the level of uncertainties of CCU models and their key process indicators that should be considered when moving on to the system level simulations and techno-economic or life cycle analyses.

Keywords: *Process modeling, Membrane separation, Methanol synthesis, Dimethyl carbonate production, Sensitivity analysis*

1. INTRODUCTION

Carbon capture has been identified as an important tool for managing carbon emissions for a long time (Reichle et al., 1999). Early studies have focused on CO_2 capture from fossil-based power generation and industrial point sources, such as steel mills. More recently, emphasis has also been given to CO_2 sources with biogenic origin, such as from biogas upgrading processes, fermentation, pulp mills and biomass fueled power plants (Rodin et al., 2020). Future possibilities also involve direct carbon capture from air as the capture technologies are developing to be more feasible also with minimal CO_2 contents and availability of green energy is increasing (Akimoto et al., 2021).

There are many possibilities for utilizing the captured CO_2 with the highest market potential existing in oil and chemical industry sectors (Koytsoumpa et al., 2018). Methanol is of particular interest in this study due to its possible use as both a fuel and as a chemical feedstock. As a fuel, methanol has advantages over directly combusting hydrogen, due to methanol's easier storability, better volumetric energy density, and compatibility to existing internal combustion engines and infrastructure (Gumber and Gurumoorthy, 2018).

Methanol can be further refined into a multitude of different hydrocarbon products including formaldehyde, methyl tert-butyl ether, acetic acid, methyl methacrylate, and dimethyl ether (Gumber and Gurumoorthy, 2018). Another derivative from methanol is dimethyl carbonate (DMC). DMC serves a multitude of purposes across diverse industries, such as a solvent for paints, coatings, and cleaning agents. DMC can be used as an additive in gasoline and diesel fuels, enhancing combustion efficiency. Moreover, DMC plays a pivotal role in the realm of energy storage, being utilized as an electrolyte component in advanced lithium-ion batteries (Kohli et al., 2022). DMC also offers a non-carcinogenic alternative to commonly used chemicals like dichloromethane and dimethyl sulfate in carbonylation and transesterification reactions. (Wei et al., 2023)

Stemming from the choice of methanol and DMC as products of interest, the modeled process chain in this work includes a membrane-based CO_2 capture unit, methanol synthesis plant unit, and a DMC reactor unit. Membranes were chosen over the more popular amine-based approach, as it shows high energy efficiency and small physical and chemical footprint (Hou et al., 2022). High-level illustration of the process chain is visible in Fig. 1. The figure depicts that the process chain takes flue gas and hydrogen as raw material feeds, and outputs methanol and DMC as the main products. It is visible in Fig. 1 that the captured CO_2 stream is divided between methanol and DMC syntheses units and that some of the produced methanol is considered as direct product along with DMC. One advantage of this kind of synthesis chain is the ability to vary the ratio of selling methanol directly to refining it into DMC, depending on current market prices.

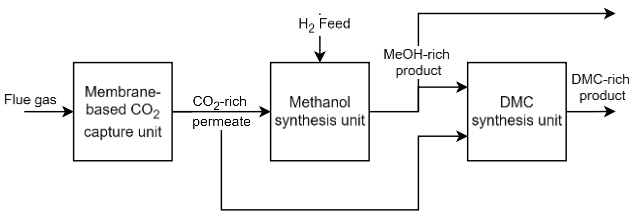

Fig. 1. Simplified diagram of the modeled CCU process chain.

The feasibility studies at system level are typically focusing on the economic profit of the production. Historical data is often available for estimating the market prices of raw materials,

products, heat, and especially the dynamical fluctuation of electricity (Karjunen et al., 2023). However, without incorporating unit level models, the system level modeling can often be limited to using constant estimates for product yield, net energy consumption, or side stream properties (Karjunen et al., 2023). Instead, these key process indicators (KPI) should preferably be treated as variables, with reasonable uncertainty ranges.

In order to assess the process performance under varying feed properties, technological limitations and uncertainties, this research aims to develop a simulation tool for the studied CCU process chain and to indicate ranges for the KPIs that can be used in system level modeling and risk assessment of an integrated CCU process. Incorporating unit level models into the system level modeling can increase the accuracy of the economical assessment by considering the effect of operation point dependencies and other sources of uncertainty in process KPIs.

2. MATERIAL AND METHODS

2.1 CO_2 capture

For the membrane-based CO_2 capture, the two-stage, pressure-driven process configuration and membrane material reported in (Asadi and Kazempoor, 2021) is considered. Namely, Polaris gen 1 membrane is assumed with permeability of CO_2 of 1000 GPU (gas permeation units, 1 GPU = $3.35 \cdot 10^{-10}$ mol/m^2/s/Pa). The selectivity between CO_2 and N_2 is 50, and the selectivity between CO_2 and O_2 is 20 (Khalilpour et al., 2012). Hollow-fiber membranes with constant dimensions are assumed, and they are operated in counter-current flow. The feed is introduced to the shell side of the membrane (outside of the fibers, retentate), and the permeate is collected from inside the membranes (bore side). The operating temperature (T), feed pressure (P), initial permeate pressure, inlet molar flowrate, recycle ratio between the membrane stages (RR), and the feed gas composition can be manipulated as well.

The modeling approach follows the reported model in (Asadi and Kazempoor, 2021) with the following exceptions:

- In addition to CO_2 and N_2, also O_2 balance is modeled.
- Feed (retentate) pressure is assumed to be constant.
- The dynamic viscosity of the gas mixture is calculated following (Wilke, 1950) applying absolute viscosities of the gas components at the operation temperature.

The process flow diagram is depicted in Fig. 2. The model also comprises the calculation of electricity consumption by the two compressors, which are modeled according to adiabatic compression equations in (Green and Southard, 2019). The process was sized by performing a constrained optimization with MATLAB® fmincon-function where the relative membrane area for the first stage, the recycle ratio of the second stage retentate to the first stage feed, and the operating pressure were determined. The second stage membrane area is assumed to be 3% of the first stage membrane area. The optimization objective was to minimize the specific energy consumption, with a penalty for deviating CO_2 purity from target 98%. This objective balances the CO_2 capture rate and energy consumption while keeping the CO_2 quality deviation within a small tolerance.

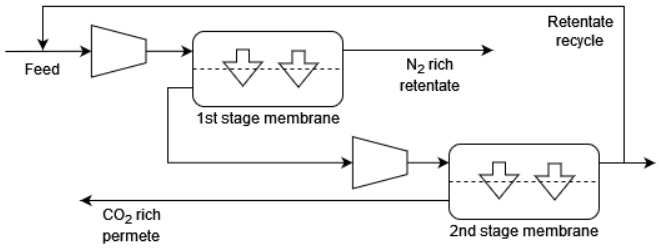

Fig. 2. Membrane-based CO_2 capture process.

2.2 Methanol synthesis

Methanol (MeOH) is generally possible to be synthetized through two overall reactions, which are the hydrogenation of CO_2 and CO (Poto et al., 2022), see (1) and (2). Reverse Water Gas Shift reaction (RWGS) is also present in the same reaction conditions (3).

$$CO_2 + 3H_2 \rightleftarrows CH_3OH + H_2O, \Delta H_0 = -49.5\ kJ/mol \quad (1)$$

$$CO + 2H_2 \rightleftarrows CH_3OH, \Delta H_0 = -90.5\ kJ/mol \quad (2)$$

$$CO_2 + H_2 \rightleftarrows CO + H_2O, \Delta H_0 = +41.2\ kJ/mol. \quad (3)$$

Heterogeneous catalysis using a $Cu/ZnO/Al_2O_3$ catalyst, in either adiabatic or isothermal reactors, is the predominately used MeOH production method in industry (Bozzano and Manenti, 2016). Due to its dominant role, $Cu/ZnO/Al_2O_3$ catalyst was also chosen for the model of this study. Even though $Cu/ZnO/Al_2O_3$ catalyst has been researched for decades, the exact roles of different reaction pathways are still debated in the literature to this day (Azhari et al., 2022). Nevertheless, for this work, the kinetic model developed in (Bussche and Froment, 1996) was chosen, due to a recommendation in (Bozzano and Manenti, 2016). The chosen kinetic model dismisses CO hydrogenation (2) to form MeOH and does not include any side reactions besides RWGS (Bussche and Froment, 1996).

For the model of this work, a Lurgi-type tube-and-shell reactor was chosen. The gas phase reactants flow through the reactor tubes that are filled with solid catalyst pellets. The shell side of the reactor has pressurized cooling water to control the reaction temperature. The purpose of cooling is to prevent the maximum temperature inside the reactor tubes from exceeding 280 °C (553 K) as the catalyst deactivates faster at high temperatures (Hartig and Keil, 1993). A steady-state pseudo-homogeneous reactor model based on mass fractions was chosen from (Manenti et al., 2011) with the following assumptions:

- Ideal plug flow (constant axial velocity, negligible axial diffusion, perfect radial mixing) (Manenti et al., 2011).
- Homogeneous gas and solid phases inside the tubes (no temperature, pressure, or composition gradient within a catalyst particle or in the surrounding gas in radial direction) (Manenti et al., 2011).
- Catalyst particle efficiency modeled by the modified Thiele modulus (Lommerts et al., 2000).

- Pressure loss inside the reactor tube modeled by the Ergun equation (Manenti et al., 2011).
- Shell side at constant bulk temperature (Manenti et al., 2011).
- Heat transfer between tube and shell modeled as in (Hartig and Keil, 1993).
- Gas density inside the reactor tube given by the Peng-Robinson equation of state (PR-EoS) (Peng and Robinson, 1976).

A process flow diagram of the modeled MeOH synthesis unit is presented in Fig. 3. In the figure, the sections surrounded by red dashed line representing the feed compression and crude methanol purification are not modeled in detail. Instead, results from (Van-Dal and Bouallou, 2013) are used to estimate the electrical and thermal energy consumptions of both unmodeled sections. Additionally, the compositions of exit streams from the crude methanol section are also estimated based on (Van-Dal and Bouallou, 2013). Most notably, this includes the product stream purity, which is assumed constant 99.9931 wt-% MeOH (Van-Dal and Bouallou, 2013). Further assumptions in the MeOH synthesis model are:

- Mixer 1 (MX1) is assumed to achieve ideal and perfect mixing of streams.
- Heat exchangers (HE) consist of bulk models, where the synthesis stream perfectly reaches the desired temperature setpoint and the model only considers the required amount of heat flow (kW). Thus, heating/cooling medium flows and temperatures are dismissed. Since sizing of heat exchangers is not considered, there are no pressure losses modeled in heat exchangers. (Parvasi et al., 2008)
- Knock out drum separator 1 (KO1) is assumed to be sized so that thermodynamic equilibrium between the liquid and gas phases is always reached. Phase equilibrium is solved using PR-EoS (Peng and Robinson, 1976), and the Rachford-Rice method (Green and Southard, 2019).
- Divisor 1 (DIV1) determines the recycle and purge stream flows based on the set maximum mass-based recycle ratio (mass flow of recycle stream divided by mass flow of feed stream). Any portion of KO1 gas effluent that exceeds the maximum recycle ratio is sent to purge stream.
- Compressor 1 (CP1) outlet pressure is fixed to the feed stream pressure. The temperature rise and electrical energy consumption of CP1 are modeled by adiabatic compression equations in (Green and Southard, 2019).

The methanol synthesis reactor was sized so that the number of reactor tubes would result the weight hourly space velocity (*WHSV*) to be equal to 4 h^{-1} at the nominal operation point, which is typical in the industry (Arab et al., 2014). In general, the model parameters were selected based on the previous studies described in the literature (Hartig and Keil, 1993; Lommerts et al., 2000; Manenti et al., 2011, 2014; Parvasi et al., 2008). The methanol synthesis model was programmed in MATLAB® and the model is publicly available at (Tiiro, 2024).

2.3 DMC synthesis

Among the DMC synthesis routes, the direct synthesis of DMC from CO_2 and methanol offers a compelling eco-friendly alternative to traditional methods. However, this pathway encounters thermodynamic hurdles stemming from the equilibrium constraints of the reaction (4):

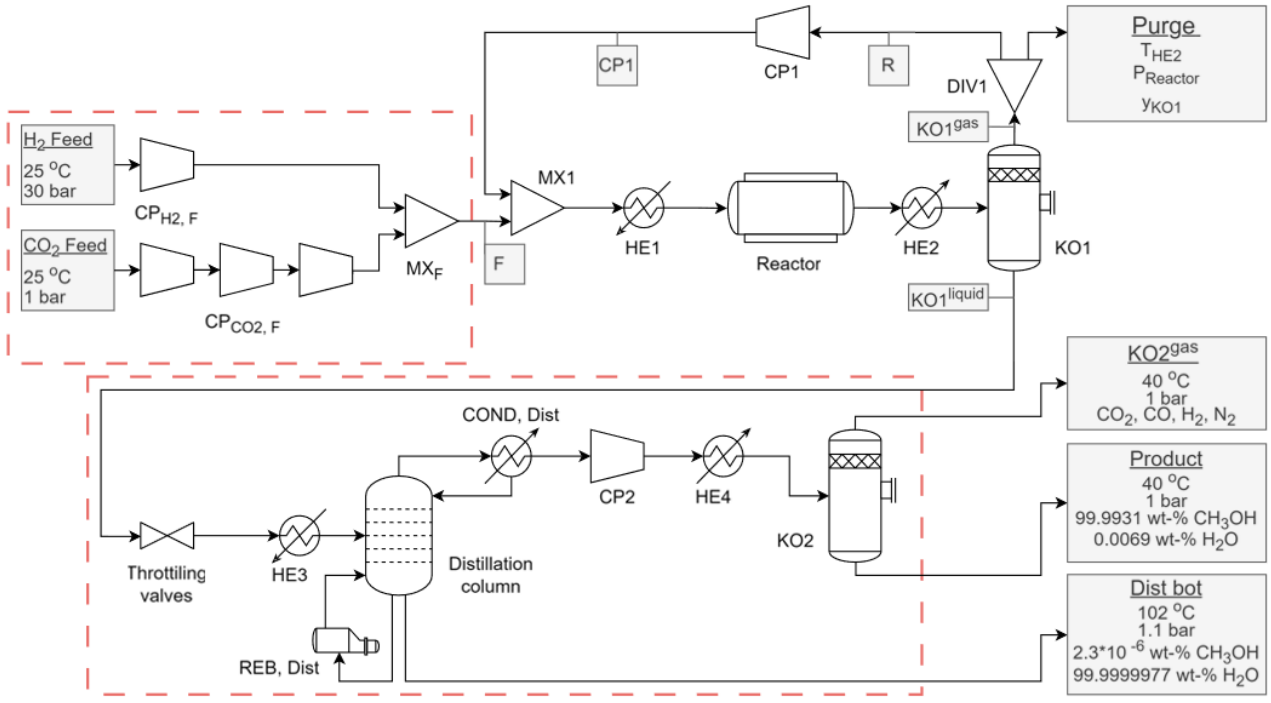

Fig. 3. Methanol synthesis process flowchart.

$$2CH_3OH + CO_2 \rightleftarrows (CH_3O)_2O + H_2O. \quad (4)$$

In addition to thermodynamic limitations, the direct DMC synthesis possesses significant challenges due to the low reactivities of both MeOH and CO_2. Consequently, catalysts play a crucial role in enhancing the efficiency of the process. In (Zheng et al., 2022), recent catalyst research is summarized, emphasizing the pivotal role of heterogeneous zirconia-based catalysts, including ZrO_2 and solid solutions of ZrO_2 with other metal oxides (M/ZrO_2).

Equations (5)–(8) detail the mass balances for each component involved in the DMC simulations. In this research, the kinetic parameters, k, were accurately fitted with the experimental data reported by (Camy et al., 2003). Differential Evolution optimization algorithm was used for the fitting.

$$\frac{dC_{CO_2}}{dt} = -k_1 C_{CO_2} \cdot C_{MeOH}^2 + k_2 C_{DMC} \cdot C_{H_2O} \quad (5)$$

$$\frac{dC_{MeOH}}{dt} = -k_3 C_{CO_2} \cdot C_{MeOH}^2 + k_4 C_{DMC} \cdot C_{H_2O} \quad (6)$$

$$\frac{dC_{H2O}}{dt} = k_5 C_{CO_2} \cdot C_{MeOH}^2 - k_6 C_{DMC} \cdot C_{H_2O} \quad (7)$$

$$\frac{dC_{DMC}}{dt} = k_7 C_{CO_2} \cdot C_{MeOH}^2 - k_8 C_{DMC} \cdot C_{H_2O} \quad (8)$$

The reaction time for the assumed sizing of the reactor in nominal operation conditions was set to 2 h. The pressure was assumed being constant, and the temperature dependence of the kinetic parameters in (5)–(8) were assumed to follow the Arrhenius equation (9):

$$k = k_0 e^{-\frac{E_A}{RT}}. \quad (9)$$

where k_0 [1/s] is the pre-exponential factor, E_A [J/mol] is the activation energy, R is the universal gas constant, and T is process temperature. The parameters are given in Table 1. The energy consumption of the direct DMC synthesis was not modeled.

Table 1. Estimated kinetic parameters for DMC synthesis.

Forward reaction		Reverse reaction	
k_{0_1}=11.31	E_{A1}=2.18·10^4	k_{0_5}=8.23	E_{A5}=1.93·10^4
k_{0_2}=3.50	E_{A2}= 1.11·10^6	k_{0_6}=12.66	E_{A6}=5.58·10^4
k_{0_3}=4.05	E_{A3}=1.57·10^4	k_{0_7}=1.70	E_{A7}=1.37·10^4
k_{0_4}=3.06	E_{A4}= 7.09·10^5	k_{0_8}=1.44	E_{A8}=2.41·10^5

3. SIMULATIONS, RESULTS, AND DISCUSSION

3.1 Simulation scenarios

For demonstrating the developed process model chain, the simulation scenarios feature CCU of pulp mill recovery boiler effluent based on (Gardarsdottir et al., 2014). In all simulation scenarios the flue gas is assumed to be first dehydrated (*e.g.* vapor-liquid separation, adsorption) from all water and cooled to 50 °C. The nominal simulation scenario (Case I), and two other scenarios to simulate the effect of feed variability to the process chain, are considered. For Case II, the flue gas has +10% molar flow and +5% CO_2 fraction. For Case III the flue gas has −10% molar flow and -5% CO_2 fraction. The flue gas flows of dried effluent, and CO_2 contents for the three scenarios are presented in Table 2.

The process designs and choices for dividing streams between units are determined and fixed based on the nominal simulation case (Case I). Fixing some of the flows in the process chain streams represents constraints that might be present in a plant due to fixed orders from customers, or due to instrument sizing. The higher flue gas flow and CO_2 content in Case II represent an undersized process design for the process chain, and the opposite, Case III represents partial load circumstances. The KPIs of especial interest in the process chain are yields and specific energy consumptions *(SEC)* of the process units.

Table 2. Flue gas properties for the different simulation scenarios.

	Case I	Case II	Case III
Flue gas flow (mol/s)	3734	4107	3361
CO_2 content (mol-%)	16.4	17.2	15.6
N_2 content (mol-%)	78.2	77.6	79.0
O_2 content (mol-%)	5.4	5.2	5.4

The process chain simulations assume the following:

- CO_2 capture is performed with a membrane-based process as described in Section 2.1. The total membrane area is 2.12·10^5 m^2, the membrane fiber outer radius is 600 µm and the inner radius is 400 µm. The operation pressure is 5 bar, temperature 50 °C and the recycle ratio is 1.
- The CO_2 rich permeate stream is divided into methanol and DMC syntheses so that 125 mol/s of permeate is always directed to the DMC synthesis and rest to the MeOH synthesis.
- Hydrogen production is not simulated, and the hydrogen feed is assumed to be perfectly pure. If the permeate stream contains oxygen, excess hydrogen is included in the MeOH synthesis feed to convert all oxygen into water. Hydrogen flow is controlled so that the MeOH synthesis feed contains 3:1 molar ratio of H_2 to CO_2 and no free oxygen.
- The MeOH synthesis is simulated as described in Section 2.2. For design parameters, the reactor tube length is 7 m, the tube inner radius is 4.2 cm, and the number of tubes is 1900. The catalyst is assumed to be fresh, and thus at 100% activity. For operational variables, the reactor inlet temperature (T_{inlet}) is 510 K, the reactor inlet pressure is 78 bar, the reactor shell side temperature (T_{shell}) is 533 K, temperature for the crude methanol separation at KO1 is 308 K, and the mass based recycle ratio (RR) is 5.
- Produced MeOH is divided into two streams. The first stream is a fixed product stream with a flow of 45 mol/s. The rest of MeOH flows to the DMC synthesis to combine with the dedicated portion of CO_2-rich permeate stream.
- The DMC synthesis is simulated according to the model in Section 2.3. The pressure is assumed to be 126 bar and the temperature 453.15 K.

3.2 Sensitivity to feed fluctuations

The resulting molar flows of products and KPIs from the three different cases are reported in Table 3. In the table, the total CO_2 efficiency is given (10):

$$\frac{\dot{n}_{MeOH,sold} + 3\,\dot{n}_{DMC,sold}}{\dot{n}_{CO2,flue\ gas}}, \quad (10)$$

where $\dot{n}_{MeOH,sold}$ combines the constant stream of 45 mol/s, and the flow of leftover MeOH after the DMC synthesis. $\dot{n}_{DMC,sold}$ represents the molar flow of produced DMC and is multiplied by 3 to account for reaction stoichiometry from CO_2. $\dot{n}_{CO2,flue\ gas}$ is the molar flow of CO_2 in flue gas stream.

In the nominal case, membrane-based CO_2 capture shows a capture efficiency of 70.1% while the CO_2 content is increased from 16.4 mol-% to 97.8 mol-%. According to Table 3, the relative change in the quality of captured CO_2 is small, less than 0.5 mol-%. The change in CO_2 capture rate in Table 3 corresponds approximately ±5% change with respect to the nominal case.

From the perspective of the MeOH synthesis, the different simulation cases have similar captured CO_2 qualities, while the permeate flowrates vary more significantly. Compared to Case I, the resulting changes to MeOH production rate in Case II and Case III are in-line with the changes to permeate flow rates (> ±10%), while changes to yield and *SEC* are much smaller (< ±1%, and < ±2%, respectively). The differences in MeOH yield and *SEC* between the cases can be explained by changes in *WHSV*. With less feed flow in Case III compared to Case I, the reactants have longer residence time in the reactor, and the pressure losses are smaller, thus allowing improved yield and *SEC*. The effects to yield and *SEC* are reversed for Case II, as *WHSV* increases compared to Case I. However, in general, it can be concluded that the MeOH production KPIs are not drastically affected by fluctuations in the feed conditions.

Nominally, the DMC production feed ratio for MeOH and CO_2 is equal to 2. With this feed composition, the DMC process shows a yield of 53.4% (on MeOH basis). For DMC, the upstream changes cause the MeOH-to-CO_2 ratio to change between 1.7 and 2.3. In addition, the fixed reactor size also means that the residence time changes due to fluctuations in the total feed flow. In Case II, the residence time is 1.83 h and in Case III 2.23 h instead of nominal value of 2 h (Case I). As presented in Table 3, longer residence time increases the DMC yield.

With respect to the total CO_2 efficiency, the partial load case represents 4% better relative efficiency than in the nominal case, as molar yields and CO_2 capture rate are all improved. On the contrary, in Case II, the overall efficiency is decreased by 5.2%.

3.3 Process chain flexibility

To study the flexibility of the process chain, it is examined if modifying the operational variables of CO_2 capture and MeOH synthesis units can compensate the lower flue gas flow and quality in Case III. The aim is to maintain the process chain throughput at the same level as in Case I, while the process design parameters remain fixed. For CO_2 capture, the goal is to provide an equal amount of CO_2 flow to downstream processes as in the nominal case, while achieving as high purity as possible. For MeOH synthesis unit, the aim is to produce an equal flow of methanol as in Case I.

The membrane-based CO_2 capture can be operated at different pressures and 2nd stage retentate recycle ratios. The increment of 1st stage operation pressure would have a significant negative effect on the *SEC* due to the very large amount of gas (flue gas and recycle) needed to be elevated into higher pressure. Thus, adjusting only the 2nd stage operation pressure, and recycle ratio are considered in this work.

Table 3. Resulting molar flows and key performance indicators in cases I to III.

	Case I	Case II	Case III
Molar flow of captured CO_2 (mol_{CO2} / s)	430	470	388
Captured CO_2 quality (mol-%)	97.8	98.2	97.4
CO_2 capture rate (mol-%)	70.1	66.4	74.0
SEC, CO_2 capture (kJ_{el} / mol_{CO2})	78.4	79.0	78.4
Ratio of captured CO_2 flowing to MeOH feed and to DMC feed (-)	2.5	2.8	2.2
Molar flow of captured CO_2 to MeOH synthesis (mol_{CO2} / s)	308	347	266
Molar flow of produced MeOH (mol_{MeOH} / s)	289	324	251
Molar yield of MeOH from CO_2 (mol-%)	94.1	93.3	94.3
SEC, MeOH synthesis (kJ_{el} / mol_{MeOH})	33.9	34.4	33.6
Molar flow of MeOH to DMC synthesis (mol_{MeOH} / s)	245	279	206
Molar ratio of MeOH and CO_2 in DMC feed (-)	2	2.3	1.7
Molar flow of produced DMC (mol_{DMC} / s)	65	69	60
Molar yield of DMC from MeOH (mol-%)	53.4	49.2	58.6
Molar flow of unreacted MeOH from DMC synthesis (mol_{MeOH} / s)	81	99	61
Total CO_2 efficiency (mol-%)	52.4	49.7	54.5

A set of simulations were performed to assess the flexibility of CO_2 capture in Case III by altering the recycle ratio and 2nd stage operation pressure. High recycle ratio is preferred to increase both the CO_2 purity and recovery. Recycle increases the feed CO_2 content and thus generates a higher driving force for the membrane separation. However, the operation pressure has opposite effects to the two KPIs, as can be seen in Fig. 4. Increasing the pressure leads to a higher recovery, but due to improved overall permeation, the quality of permeate decreases linearly. In terms of energy consumption, the higher 2nd stage pressure, and thus capture rate, results in lower *SEC* (in 9 bar, 73.6 kW/molCO2). Finally, in the partial load case, the target CO_2 flow (equal to Case I) could be achieved with the 2nd stage operation pressure of 11.5 bar (extending from the range seen in Fig. 4). In these conditions, the CO_2 purity was only 91.3 mol-%, the CO_2 recovery 82.0%, and the total molar flow rate 471 mol/s. The resulting total flow rate would be 7.2% higher than in Case I, meaning that the downstream processes will need to handle a larger amount of gas than expected by the nominal design, requiring more flexibility from them.

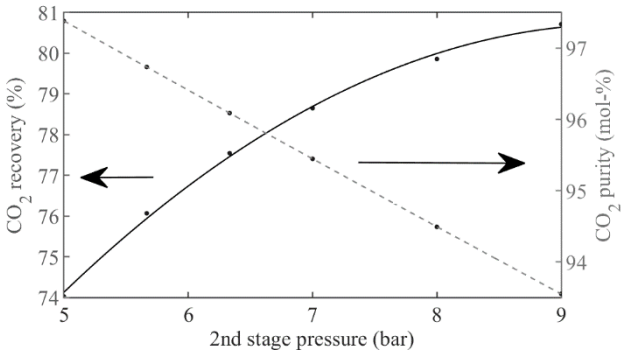

Fig. 4. The effect of operation pressure on the CO_2 capture performance. The recycle ratio is 1.

Thus, it can be concluded that the selected operation variables in the CO_2 capture cannot solely compensate for the flue gas variations in the partial load case. The disturbances are partly propagated to the downstream processes resulting in 337 mol/s of permeate flowing to MeOH synthesis and 134 mol/s of permeate to the DMC synthesis with decreased purity as described earlier. It should be noted that the gas membrane systems can be designed as modular units. Thus, increased flexibility can be achieved by altering the effective membrane area (number of active modules) to maintain the performance characteristics.

For flexibility in MeOH synthesis unit, it was seen that there are three operational variables, that can be most easily manipulated to adjust the production rate: Reactor inlet temperature (T_{inlet}), reactor shell side temperature (T_{shell}), and recycle ratio (*RR*). There were no constraints set to the operational variables, other than that the resulting temperature should not exceed the earlier mentioned temperature limit of 553 K at any point along the reactor tubes.

By performing global optimization using differential evolution algorithm from (Buehren, 2024), a set of operational variables was found that results in practically equal MeOH production rate (289 mol/s) as in the nominal case: T_{inlet} = 505.2 K, T_{shell} = 534.1 K, and *RR* = 11.19. Expectedly, with such a high recycle stream, *SEC* is noticeably higher (40.0 kJ_{el} / mol_{MeOH}) compared to the nominal case (33.9 kJ_{el} / mol_{MeOH}). The found operational point does demonstrate that the MeOH synthesis plant can be operated flexibly to compensate even for major changes in the captured CO_2 purity. Thus, the membrane-based CO_2 capture unit and the MeOH synthesis unit combined can fully compensate for the feed variability of the studied scenarios, so that the DMC production and the overall productivity of the process chain is unaffected.

However, it is worth mentioning that the operational variable values for the MeOH synthesis in the flexibility case are considerably above their normal ranges that can be found in the literature. The reason why using so large temperatures and a recycle ratio does not cause operational issues within the simulations, can likely be attributed to the simplifications present in the MeOH synthesis model. By including currently unmodeled phenomena, such as limitations to radial heat transfer inside reactor tubes (Hartig and Keil, 1993), or pressure losses taking place in heat exchangers, such an extreme operation point might become unviable.

3.4 Implications to techno-economic analyses

The ongoing debate in the scientific literature for the kinetics of methanol synthesis reactions is one major source of uncertainty for modeling the MeOH production. To examine sensitivity of the MeOH synthesis towards chosen reaction kinetics, Case I was simulated with an updated kinetic parameter set reported in (Mignard and Pritchard, 2008). The simulation resulted in the flow of produced methanol rising from 289 to 298 mol/s. Methanol yield from CO_2 rose from 94.1 to 96.7 mol-%. *SEC* decreased from 33.9 to 33.0 kJ_{el} / mol_{MeOH}. The changes in these KPIs are significant even though the update from (Mignard and Pritchard, 2008) is only altering two of the parameters in the kinetic model of (Bussche and Froment, 1996). It could be speculated that modeling the reaction kinetics after a completely different model structure, such as in (Graaf et al., 1988), could cause even more significant changes to the KPIs. In general, the same principle applies for the kinetics in the DMC production, and the permeabilities and selectivities of different membrane materials.

As demonstrated by the flexibility simulations, the choice of operational variables carries a significant effect on the product purity, yield and *SEC* in the different unit processes, meaning that choosing an optimal operation point is also important at system level analyses. For example, methanol synthesis in Case I was simulated with the highest reactor inlet and shell side temperatures found from the used literature. If the same case is instead simulated with significantly lower temperatures (T_{inlet} = 484 K, T_{shell} = 520 K), from (Manenti et al., 2014), then the flow of produced methanol lowers by 5.5% to 273 mol/s, the methanol yield from CO_2 drops to 88.7 mol-%, whilst *SEC* rises to 35.7 kJ_{el} / mol_{MeOH}.

For the DMC production, the estimates are uncertain due to the low technology readiness level and lab-scale data. In general, the direct DMC synthesis is very energy intensive (*e.g.* 19.2

MJ/mol under process conditions T = 323.15 K and P = 150 bar (Saavalainen et al., 2015)). To enhance the yield of DMC, Zheng et al. (2022) implemented a natural convection circulation system specifically to adsorb and remove water.

Models can also give overly optimistic estimates due to their inability to account for uncertainties in geometry. For example, the hollow-fiber membrane model assumed a fixed inner and outer radius, although real systems with thousands or millions of fibers might have variability in their properties. It has been shown that the standard deviation over 10% in fiber geometry can have a significant impact on the CO_2 recovery (Bocciardo, 2015). The sensitivity of the geometry parameters in CO_2 capture was also observed in this study. For instance, simulating Case I with a 2.5% decrement in both membrane fiber radius values leads to CO_2 purity lowering from 97.8 to 97.6%, capture rate lowering from 70.1 to 69.2%, and *SEC* rising from 78.4 to 82.0 kJ_{el} / mol_{CO2}. Moreover, MeOH and DMC production efficiencies are also greatly dependent on the reactor dimensions.

Yet another factor to be accounted for is the long-term stability of the processes. The membrane-based CO_2 capture has shown good stability in extended periods of operation for coal-fired combustion flue gases (Cui et al., 2021). On the other hand, an industrial data-based study suggests that the activity of $Cu/ZnO/Al_2O_3$ catalyst in methanol synthesis can drop to 65% when the catalyst has operated for 100 days, and further reduce to 50% after a year of operation (Parvasi et al., 2008). Thus, focusing solely on the performance of fresh catalyst, as has been done in this study, can result in overly optimistic KPIs. If simulating Case I otherwise unchanged, but the catalyst activity is at 50%, the flow of produced methanol drops to 228 mol/s. The methanol yield from CO_2 lowers to 74.2 mol-%, and *SEC* rises to 42.6 kJ_{el} / mol_{MeOH}. The matter is relevant considering that the average lifetime of $Cu/ZnO/Al_2O_3$ catalyst is 3 to 4 years (Bozzano and Manenti, 2016).

4. CONCLUSIONS

In this work a CCU process chain involving membrane-based CO_2 capture, MeOH synthesis and DMC synthesis was modeled. In simulations it was found that the studied CCU process chain is quite robust against feed fluctuations, and by operating the membrane-based CO_2 capture unit and the MeOH synthesis flexibly together, it was possible to fully compensate the decrease in the production rate in the studied worst case feed conditions. More importantly for techno-economic analysis, it was discovered that the CCU process chain is significantly more sensitive to model parameters than to feed variations.

Furthermore, the significant changes to yields and specific electricity consumptions from varying operational variables and design parameters imply that considering their optimal choice should play a significant role also in system level studies. Thus, for techno-economic analyses of CCU processes it is crucial to find profit-wise optimum solutions that balance various factors, such as investment costs versus operating costs when sizing equipment, or yield versus catalyst life when choosing synthesis temperatures. Access to industrial data from relevant operation conditions would be highly valuable for increasing the reliability of the process models.

ACKNOWLEDGEMENTS

This work was funded by Business Finland via project 'Bio-CCU - Creating sustainable value of the bio-based CO_2' (2352/31/2022).

REFERENCES

Akimoto, K., Sano, F., Oda, J., Kanaboshi, H., and Nakano, Y. (2021). Climate change mitigation measures for global net-zero emissions and the roles of CO2 capture and utilization and direct air capture. *Energy and Climate Change*, *2*, 100057.

Arab, S., Commenge, J.-M., Portha, J.-F., and Falk, L. (2014). Methanol synthesis from CO2 and H2 in multi-tubular fixed-bed reactor and multi-tubular reactor filled with monoliths. *Chemical Engineering Research and Design*, *92*(11), 2598–2608.

Asadi, J., and Kazempoor, P. (2021). Techno-economic analysis of membrane-based processes for flexible CO2 capturing from power plants. *Energy Conversion and Management*, *246*, 114633.

Azhari, N. J., Erika, D., Mardiana, S., Ilmi, T., Gunawan, M. L., Makertihartha, I. G. B. N., and Kadja, G. T. M. (2022). Methanol synthesis from CO2: A mechanistic overview. *Results in Engineering*, *16*, 100711.

Bocciardo, D. (2015). *Optimisation and integration of membrane processes in coal-fired power plants with carbon capture and storage*. University of Edinburgh.

Bozzano, G., and Manenti, F. (2016). Efficient methanol synthesis: Perspectives, technologies and optimization strategies. *Progress in Energy and Combustion Science*, *56*, 71–105.

Buehren, M. (2024). *Differential Evolution* (https://www.mathworks.com/matlabcentral/fileexchange/18593-differential-evolution; 1.16.0.1) [MATLAB]. MATLAB Central File Exchange.

Bussche, K. M. V., and Froment, G. F. (1996). A Steady-State Kinetic Model for Methanol Synthesis and the Water Gas Shift Reaction on a Commercial Cu/ZnO/Al2O3Catalyst. *Journal of Catalysis*, *161*(1), 1–10.

Camy, S., Pic, J.-S., Badens, E., and Condoret, J.-S. (2003). Fluid phase equilibria of the reacting mixture in the dimethyl carbonate synthesis from supercritical CO2. *The Journal of Supercritical Fluids*, *25*(1), 19–32.

Cui, Q., Wang, B., Zhao, X., Zhang, G., He, Z., Long, Y., Sun, Y., and Ku, A. Y. (2021). Post-combustion slipstream CO2-capture test facility at Jiangyou Power Plant, Sichuan, China: Performance of a membrane separation module under dynamic power-plant operations. *Clean Energy*, *5*(4), 742–755.

Gardarsdottir, S. O., Normann, F., Andersson, K., and Johnsson, F. (2014). Process Evaluation of CO2 Capture in three Industrial case Studies. *Energy Procedia*, *63*, 6565–6575.

Graaf, G. H., Stamhuis, E. J., and Beenackers, A. A. C. M. (1988). Kinetics of low-pressure methanol synthesis. *Chemical Engineering Science*, *43*(12), 3185–3195.

Green, D. W., and Southard, M. Z. (Eds.). (2019). *Perry's Chemical Engineers' Handbook 9th Edition* (Ninth edition). McGraw Hill Education.

Gumber, S., and Gurumoorthy, A. V. P. (2018). Methanol Economy Versus Hydrogen Economy. In *Methanol* (pp. 661–674). Elsevier.

Hartig, F., and Keil, F. J. (1993). Large-scale spherical fixed bed reactors: Modeling and optimization. *Industrial and Engineering Chemistry Research*, *32*(3), 424–437.

Hou, R., Fong, C., Freeman, B. D., Hill, M. R., and Xie, Z. (2022). Current status and advances in membrane technology for carbon capture. *Separation and Purification Technology*, *300*, 121863.

Karjunen, H., Tynjälä, T., Kuparinen, K., Vakkilainen, E., and Joronen, T. (2023). Value creation by converting pulp mill flue gas streams to green fuels. *TAPPI Journal*, *22*(3), 193–205.

Khalilpour, R., Abbas, A., Lai, Z., and Pinnau, I. (2012). Modeling and parametric analysis of hollow fiber membrane system for carbon capture from multicomponent flue gas. *AIChE Journal*, *58*(5), 1550–1561.

Kohli, K., Sharma, B. K., and Panchal, C. B. (2022). Dimethyl Carbonate: Review of Synthesis Routes and Catalysts Used. *Energies*, *15*(14), 5133.

Koytsoumpa, E. I., Bergins, C., and Kakaras, E. (2018). The CO2 economy: Review of CO2 capture and reuse technologies. *The Journal of Supercritical Fluids*, *132*, 3–16.

Lommerts, B. J., Graaf, G. H., and Beenackers, A. A. C. M. (2000). Mathematical modeling of internal mass transport limitations in methanol synthesis. *Chemical Engineering Science*, *55*(23), 5589–5598.

Manenti, F., Cieri, S., and Restelli, M. (2011). Considerations on the steady-state modeling of methanol synthesis fixed-bed reactor. *Chemical Engineering Science*, *66*(2), 152–162.

Manenti, F., Leon-Garzon, A. R., Ravaghi-Ardebili, Z., and Pirola, C. (2014). Systematic staging design applied to the fixed-bed reactor series for methanol and one-step methanol/dimethyl ether synthesis. *Applied Thermal Engineering*, *70*(2), 1228–1237.

Mignard, D., and Pritchard, C. (2008). On the use of electrolytic hydrogen from variable renewable energies for the enhanced conversion of biomass to fuels. *Chemical Engineering Research and Design*, *86*(5), 473–487.

Parvasi, P., Rahimpour, M. R., and Jahanmiri, A. (2008). Incorporation of Dynamic Flexibility in the Design of a Methanol Synthesis Loop in the Presence of Catalyst Deactivation. *Chemical Engineering and Technology*, *31*(1), 116–132.

Peng, D.-Y., and Robinson, D. B. (1976). A New Two-Constant Equation of State. *Industrial and Engineering Chemistry Fundamentals*, *15*(1), 59–64.

Poto, S., Vico Van Berkel, D., Gallucci, F., and Fernanda Neira d'Angelo, M. (2022). Kinetic modelling of the methanol synthesis from CO2 and H2 over a CuO/CeO2/ZrO2 catalyst: The role of CO2 and CO hydrogenation. *Chemical Engineering Journal*, *435*, 134946.

Reichle, D., Houghton, J., Kane, B., Ekmann, J., and Others, A. (1999). *Carbon sequestration research and development* (DOE/SC/FE-1). Oak Ridge National Lab. (ORNL), Oak Ridge, TN (United States); National Energy Technology Lab., Pittsburgh, PA (US); National Energy Technology Lab., Morgantown, WV (US).

Rodin, V., Lindorfer, J., Böhm, H., and Vieira, L. (2020). Assessing the potential of carbon dioxide valorisation in Europe with focus on biogenic CO2. *Journal of CO2 Utilization*, *41*, 101219.

Saavalainen, P., Kabra, S., Turpeinen, E., Oravisjärvi, K., Yadav, G. D., Keiski, R. L., and Pongrácz, E. (2015). Sustainability Assessment of Chemical Processes: Evaluation of Three Synthesis Routes of DMC. *Journal of Chemistry*, *2015*, 1–12.

Tiiro, K. (2024). *krti01github/Modeling-methanol-synthesis-plant-in-Matlab: V1.0.0* (v1.0.0) [MATLAB]. doi:10.5281/ZENODO.11121416

Van-Dal, É. S., and Bouallou, C. (2013). Design and simulation of a methanol production plant from CO2 hydrogenation. *Journal of Cleaner Production*, *57*, 38–45.

Wei, W., Wang, Y., Yan, Z., Hou, J., Xu, G., and Shi, L. (2023). One-step DMC synthesis from CO2 under catalysis of ionic liquids prepared with 1,2-propylene glycol. *Catalysis Today*, *418*, 114052.

Wilke, C. R. (1950). A Viscosity Equation for Gas Mixtures. *The Journal of Chemical Physics*, *18*(4), 517–519.

Zheng, Q., Nishimura, R., Sato, Y., Inomata, H., Ota, M., Watanabe, M., and Camy, S. (2022). Dimethyl carbonate (DMC) synthesis from methanol and carbon dioxide in the presence of ZrO2 solid solutions and yield improvement by applying a natural convection circulation system. *Chemical Engineering Journal*, *429*, 132378.